Anais XIV Simpósio Brasileiro de Sensoriamento Remoto, Natal, Brasil, 25-30 abril 2009, INPE, p. 451-458.

Analyses of the evaporative fraction using eddy covariance and remote sensing techniques

Carlos Antonio Costa dos Santos[1,2]
Bernardo Barbosa da Silva[1]
Christopher Michael Usher Neale[2]

[1] Department of Atmospheric Science, Federal University of Campina Grande, Avenida Aprígio Veloso, 882, Bodocongó, Campina Grande, PB, CEP: 58109-970, Brazil
carlostorm@gmail.com/ bernardo@dca.ufcg.edu.br
[2] Biological and Irrigation Engineering Department, Utah State University, 4105 Old Main Hill, Logan, UT 84322, USA
cneale@cc.usu.edu

Abstract: The main objective of this study was apply the remote sensing algorithm (SEBAL) to estimate the regional distribution of the instantaneous EF using the combination of Landsat-5 TM scenes and eddy covariance measurements to validate the results. This experimental campaign was conducted in Ceará State, Brazil, in banana orchard of Frutacor farm. This study used 4 Landsat – 5TM images, to application of SEBAL algorithm. The results evidenced that, in the studied area, it is indifferent use images from satellite that has morning or afternoon overpass to obtain the EF. In analyses of the EF maps over the studied area have been identified the behavior of different targets. The derived EF in four different images over the study area showed, in general, good agreement with measured data.

Keywords: Evapotranspiration, banana crop, semiarid, SEBAL, evapotranspiração, cultura da banana, SEBAL

1 – Introduction

Estimates of evapotranspiration (ET) are of crucial need for climatic studies, weather forecasts, ecological monitoring, hydrological surveys, and water resource management (Bastiaanssen et al., 2000). Within semiarid agricultural regions, which hydrological cycle is strongly influenced by ET through crop water consumption, a precise ET estimation is of importance for water saving through efficient irrigation practices (Hoedjes et al., 2008). However, in practice, continuous daily ET measurements are rarely available (Farah et al., 2004). Remote sensing techniques offer means of estimating actual ET at a large spatial scale, which is not possible with the traditional point methods. A fundamental problem in using remote sensing to estimate the ET in local and regional scales is the scaling of instantaneous latent heat flux (LE) to daily ET. Because remotely sensed data for this purpose, in general, are provided by satellite or airborne platforms (Colaizzi et al., 2006). Chávez et al. (2005) explain that in the use of satellite imagery there are other important things to consider, such the spatial resolution, overpass frequency, cloud cover presence at overpass time, etc., which sometimes limits the application. Many techniques have been proposed to solve the surface energy balance from remote sensing (Bastiaanssen et al., 1998; Roerink et al., 2000). However, remote sensing data are instantaneous measurements and a method is required to temporally integrate instantaneous estimates of ET.

The components of the energy balance display considerable diurnal variation over land surfaces (Farah et al., 2004). Recently, the evaporative fraction (EF) has been found to have a little variation during daytime, although it is directly related to Bowen ratio (β)

(Crago and Brutsaert, 1996; Gentine et al., 2007), the diurnal behavior of EF can be understood from its relationship with atmospheric conditions and surface characteristics. Crago (1996) affirms that under clear days, the steadiness and predictability of the daytime cycle of radiation, heat, and humidity tend to cause the components of the energy balance to vary rather slowly. In addition, some simple ratios of energy balance components, most prominently the EF, tend to have little variation during the daytime. The evaporative fraction is defined as:

$$EF = \frac{LE}{R_n - G} = \frac{LE}{LE + H} = \frac{1}{1 + \beta} \quad (1)$$

where LE is the latent heat flux, R_n is the net radiation, H is the sensible heat flux, and G is the soil heat flux.

The purpose of this paper is apply the remote sensing algorithm (SEBAL) to estimate the regional distribution of the instantaneous EF using the combination of Landsat-5 TM scenes and ground-based data by eddy covariance measurements to validate the results.

2 – Materials and Methods

2.1 – Site description

The study area was located in the irrigation district of Quixeré in Low Jaguaribe basin, Ceará, Brazil. The instruments was installed in the Frutacor farm, with approximate area of 250 ha of banana crop (*Musa sp*.) located at 5º08'44"S and 38º05'53"W, presenting elevation of 147.0 m, approximately. The referred area is illustrated in **Figure 1a**. The spacing between rows and plants was 4.0 m and 2.4 m, respectively, and the plants height was of 5.0 m, this area is irrigated by drip subsurface. The area presents semi-arid climate, type BSw'h', in agreement with the Köeppen climatic classification. Mean annual temperature is 28.5ºC, being the mean maximum and minimum annual temperature of 36ºC and 22ºC, respectively. The mean annual precipitation is 772 mm, based on monthly mean distribution for 25 years (1981 - 2006) registered in the Quixeré weather station; it is illustrated in the **Figure 1b**. The mean annual potential evaporation is 3,215 mm and the mean relative humidity annual is 62%.

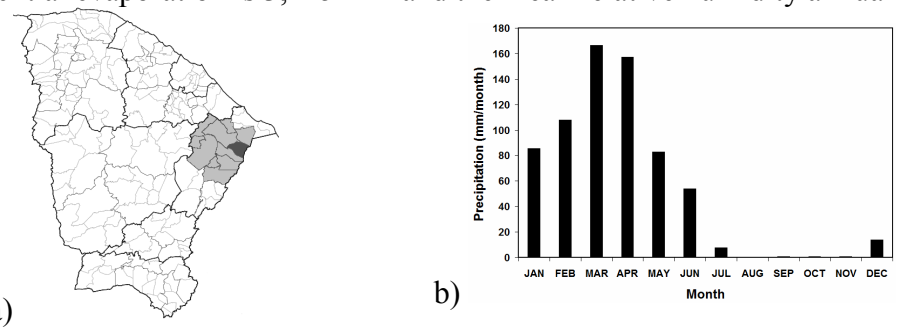

Figure 1: a) Location of the Low Jaguaribe basin and the irrigation district of Quixeré; **b**) Distribution of the monthly averages of the precipitation in Quixeré (1981 – 2006).

2.2 – Methods

The data was collected during the months from October/2005 to September/2006. The climatic data was provided by an automatic weather station (106 Weather Station, Campbell Scientific Inc., Logan, UT, USA); these data was used to obtain the reference evapotranspiration (ET_o) by combined FAO – Penman-Monteith method (Allen et al.,

1998). The net radiation (R_n) was computed using the four components (Eq. 2) and acquired with one net radiometer (model CNR1, Kipp & Zonnen, Delf, The Netherlands) at a 7.0 m above the ground level and 2.0 m above the crop canopy in the rows (Table 1). The soil heat flux (G) was measured with two heat flux plates (model HFP01SC-L, Campbell Scientific, Inc., Logan, UT) at 2.0 cm soil depth. Flux plates were buried between rows and plants; the values of the G were obtained as the average of the two measurements.

$$R_n = S_{solar} - S_{ref} + L_{atm} - L_{surface} \quad (2)$$

where S_{solar} is the global solar radiation, S_{ref} is the reflective radiation flux, L_{atm} is the incoming longwave radiation flux and $L_{surface}$ is the outgoing long-wave radiation flux (Bastiaanssen et al., 1998). The air temperature and relative humidity were measured using a Vaisala HMP45C probe.

To obtain the turbulent flux measurements were used the eddy covariance (EC) system, composed by a fast-response open-path infrared gas analyzer (model LI-7500, Licor, Inc., Lincoln, NE) to measure CO_2 and H_2O, coupled with a three-dimensional sonic anemometer (model CSAT-3, Campbell Scientific, Inc., Logan, UT), used to measure wind speed components fluctuations, every one installed at 7.0 m above ground level (**Figure 2b**). Digital signals from these instruments were recorded at 10 Hz and the average was obtained over a 30 minutes time using a Campbell Scientific CR23X datalloger, where the data were archived for later processing.

Giolia et al. (2004) affirm that this technique provides a unique opportunity to measure the surface energy fluxes directly. The use of this technique is problematic when the gradient of the specific humidity, and thus the latent heat flux, is very small (Kalthoff el al., 2006). The EC technique measures the turbulent fluxes by measuring the fluctuations around a long-term mean, i.e. the sensible heat flux has been calculated according the following equation:

$$H = \bar{\rho} c_p \overline{w'T'} \quad (3)$$

and the latent heat flux using the equation:

$$LE = \bar{\rho} L \overline{w'q'} \quad (4)$$

where the overbar in the Eqs. (3) and (4) denotes the time average of 30 min, ρ is the air density (kg m^{-3}), w' the vertical wind speed fluctuation (m s^{-1}), T' the air temperature fluctuation (^oC), q' the specific humidity fluctuation (deviations from the 30 min average), and L is the latent heat of water ($2.508x10^6$ J kg).

To applications of the remote sensing algorithm were used 4 images from Landsat 5 - TM satellite, referring to the path 216 and row 64. These images were used to process the intermediate parameters from which surface energy flux components that were estimated.

2.2.1 – Remote sensing algorithm

Surface energy fluxes require energy inputs, moisture conditions of soil and vegetation and surface microclimate conditions. Remote sensing has proven to provide the energy inputs through the shortwave and longwave radiation and surface moisture conditions of soil and vegetation at reasonable spatial and temporal scales (Bastiaanssen et al., 1998). The surface microclimate can be obtained from meteorological stations.

The surface energy budget satisfying the law of conservation of energy in the absence of horizontally advective energy can be expressed as:

$$R_n = H + LE + G \quad (5)$$

The Surface Energy Balance Algorithms for Land (SEBAL) (Bastiaanssen et al., 1998) model utilizes remotely sensed data to solve the Eq. (5) by computing surface energy fluxes from satellite images and weather data. Application details are given in Bastiaanssen et al. (1998). The computation of R_n for each pixel is using albedo and transmittances obtained from shortwave bands and using longwave emission computed from the thermal band (**Figure 2**). The G in these algorithms is determined through semi-empirical relationships with R_n, surface albedo, surface temperature, and vegetation index (Bastiaanssen et al., 1998; Bastiaanssen, 2000):

$$G = \frac{T - 273.16}{\alpha}(0.0038\alpha + 0.0074\alpha^2)(1 - 0.98NDVI^4)R_n \quad (6)$$

where $NDVI$ is the Normalized Difference Vegetation Index computed from red and NIR bands, T (K) is radiometric surface temperature computed from the thermal band using a modified Planck equation, and α is the surface albedo.

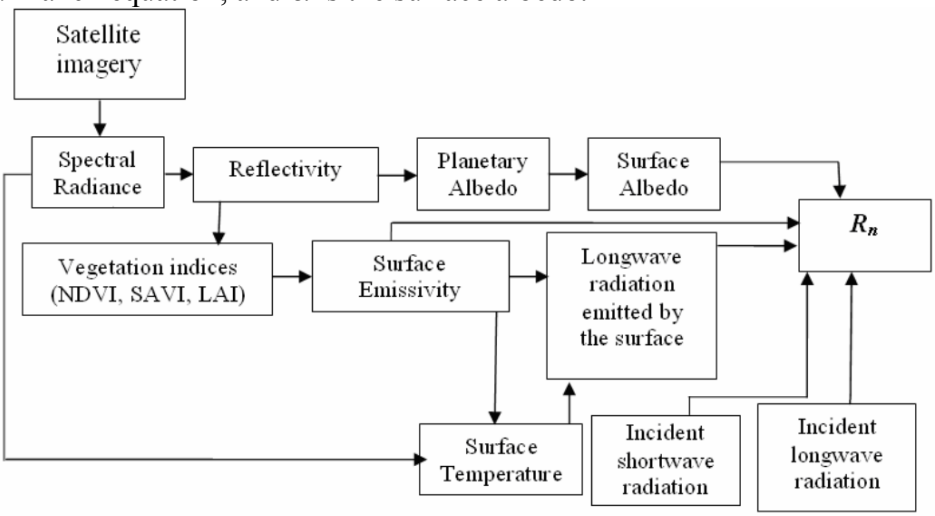

Figure 2: Flowchart of computational steps involved in obtaining R_n by SEBAL.

The obtaining of H through of SEBAL algorithm needs measurements of the wind speed at a known height and surface temperature pixel by pixel using an internal calibration of temperature difference of the air near the surface as described by Bastiaanssen et al. (1998):

$$H = \frac{\rho_{air} c_p (a + bT_s)}{r_{ah}} \quad (7)$$

where ρ_{air} is the humid air density (kg m^{-3}), c_p is the specific heat of air at constant pressure (1005 J kg^{-1} K^{-1}), r_{ah} is the aerodynamic resistance to heat transport (s m^{-1}), T_s is the surface temperature (K) and a and b are empirical calibration coefficients obtained for each image. The term (a+bT_s) or dT (K) (Bastiaanssen et al., 1998) presented in Eq. 7 is the temperature difference close the surface calculated between the 0.1 and 2.0 m heights. The definition of a and b coefficients requires choice of the two pixels, representing the extremes conditions of temperature and humidity, called the *hot* and *cold* pixels, where dT was calculated using the known values of H for these cited pixels.

For the cold pixel, chosen over an irrigated area, H is assumed to be zero and, consequently $dT = 0$ and $LE = R_n - G$. The hot pixel was chosen over an area of bare soil, where $LE = 0$ and the H value is calculated from the difference $H = R_n - G$ and $dT = H\, r_{ah}/\rho_{air}\, c_p$. Such H initial values do not represent adequately the real value of H for each pixel and serving only as the initial parameters of an iterative process (Bastiaanssen et al., 1998), in which it is considered the stability conditions of each pixel. To correct the buoyancy effect is applied the similarity theory of Monin-Obukhov, based in Monin-Obukhov length (L), as presented in the following equation:

$$L = -\frac{\rho_{air} c_p u_*^3 T_s}{kgH} \tag{8}$$

where u_* is the friction velocity of each pixel in the image (m s^{-1}), g is the gravity acceleration (9.81 m s^{-2}), and k is the von Karman constant, pixel by pixel, obtained initially considering a neutral stability condition.

To identify the stability conditions is necessary to analyze the L values given as follows: if $L < 0$, the atmosphere is considered to be stable; if $L = 0$ is considered neutral; and $L > 0$ is considered unstable. Depending of the atmospheric conditions, the values of the stability corrections, for the momentum transport (ψ_m) and the heat transport (ψ_h) must be considered as given in Bastiaanssen et al. (1998) and Bastiaanssen (2000). When is reached the final sensible heat flux the LE is obtained solving the Eq. 5. The detailed technique for estimating latent and sensible heat fluxes using remote sensing has been documented and tested in Europe, Asia, Africa, and Idaho in the USA and proved to provide good results (Bastiaanssen et al., 1998; Bastiaanssen, 2000; Melesse et al., 2008).

In summary, the latent heat flux describes the amount of energy required to maintain a certain crop evapotranspiration rate. Surface albedo, surface temperature and vegetation index are derived from satellite measurements and are used together to solve R_n, G and H. Surface temperature is an important parameter for the computation of the sensible heat flux, H. The latent heat flux, LE, is the residual term and is used to compute the instantaneous evaporative fraction (EF_{inst}):

$$EF_{inst} = \frac{LE_{inst}}{R_{n\_inst} - G_{inst}} \tag{9}$$

The instantaneous EF is an expression to obtain the evapotranspiration when the atmospheric moisture conditions are in equilibrium with the soil moisture conditions (Bastiaanssen et al., 1998). Such the evaporative fraction is temporally constant, the difference between instantaneous EF at the moment of satellite overpass and the EF derived from the 24-hour integrated energy balance is marginal, and can be neglected.

3 - Results and discussion

3.1. Diurnal behavior of EF

The relationships between morning EF, midday EF and average daytime EF are presented in **Figure 3a** and **3b**, respectively. The complete time series of micrometeorological data was used to obtaining these results. There is a moderate relationship between morning EF and daily EF ($r^2 = 0.56$), and showing better results to relationship between midday EF and daily EF ($r^2 = 0.68$). The root mean square errors (RMSE) are 0.06 and 0.05 for morning EF and midday EF, respectively. The implication

of these results for remote sensing applications is that it is indifferent for satellite that has morning overpass (for example, Landsat) or afternoon overpass (for example, NOAA AVHRR) because the results showed close results, for the studied area.

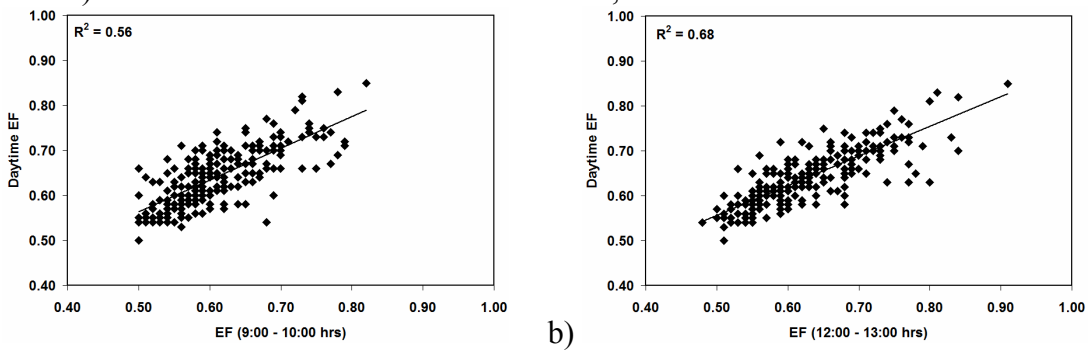

Figure 3: Correlations between daytime EF and morning EF (**a**), and between daytime EF and midday EF (**b**).

3.2. Evaporative fraction and remote sensing applications

Figure 4 shows the spatial distribution of EF over the partly heterogeneous surface of the semiarid region area obtained by remote sensing algorithm (SEBAL). These maps cover irrigated area and native vegetation (Caatinga forest) with emphasize to banana orchard, the experimental area. It is possible identify in **Figure 4**, the irrigated areas like center pivot and rectangular plots with high values of EF, native vegetation presenting medium values to EF, and bare soil showing low values of EF. The evaporative fractions derived from Landsat-5 TM scenes were compared with field measurements, as presented in **Table 1**.

The derived EF in the four different images over the study area showed, in general, good agreement with measured data. The images 10/24/2005 (**Figure 4a**), 01/28/2006 (**Figure 4b**) and 08/24/2006 (**Figure 4d**) showed absolute percent difference with the measured values of 11.0, 3.0 and 3.3%, respectively. However, in the image of 08/08/2006 (**Figure 4c**) the results presented an absolute percent difference of 36.8%. This difference could be due clouds contamination before the satellite overpass that decreased the measured EF, and how the eddy covariance system in the field presented average in each 30 minutes, a cloud contamination can be computed in the stored data.

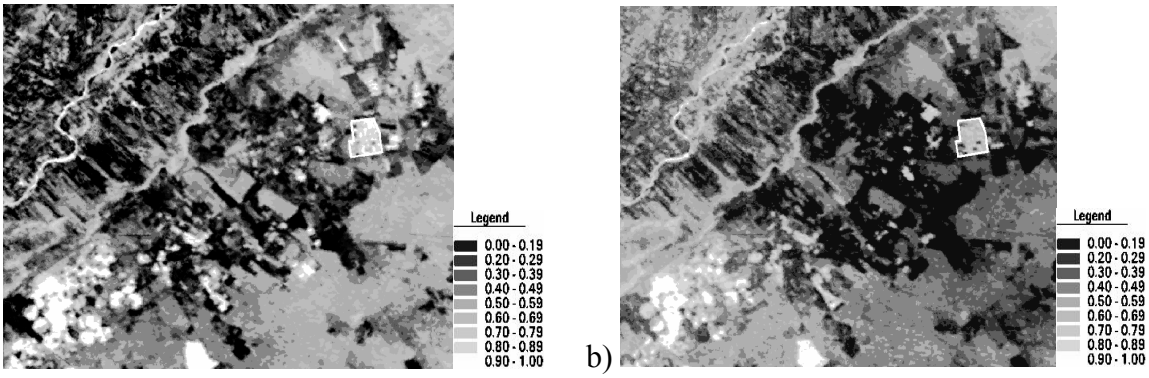

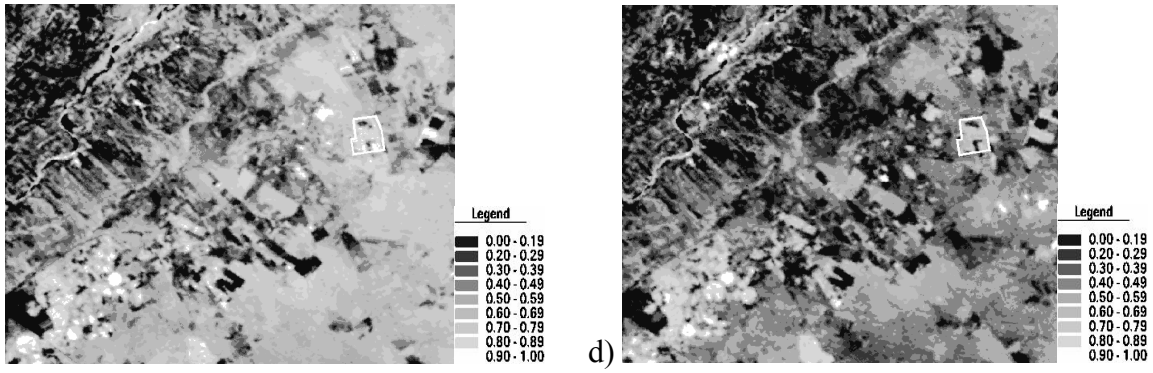

Figure 4: Spatial distribution of instantaneous evaporative fraction estimated by SEBAL, in 10/24/2005 (**a**), 01/28/2006 (**b**), 08/08/2006 (**c**) and 08/24/2006 (**d**), to semiarid region of Brazil, with highlight to banana orchard area.

Table 1: Comparison between measured EF by eddy covariance technique and estimated EF using remote sensing algorithm (SEBAL) to banana orchard

DATE	Estimated EF (SEBAL)	Measured EF (eddy covariance)	Absolute percent difference (%)
10/24/2005	0.72	0.65	11
01/28/2006	0.65	0.67	3.0
08/08/2006	0.78	0.57	36.8
08/24/2006	0.63	0.61	3.3

4 – Conclusions

This study presents analyzes of the evaporative fraction (EF) obtained by eddy covariance method, measured in a banana orchard, and comparisons among this results and values obtained through of SEBAL algorithm. The relationships between morning EF, midday EF and average daytime EF indicate that there is a moderate relationship between morning EF and daily EF and showed better results to relationship between midday EF and daily EF. Those results evidenced that, in the studied area, it is indifferent use images from satellite that has morning overpass (for example, Landsat) or afternoon overpass (for example, NOAA AVHRR) to obtain the EF, because the results showed close values. In analyses of the EF maps over the studied area have been identified the irrigated areas such center pivot and rectangular plots with high values of EF, native vegetation presenting medium values to EF, and bare soil showing low values of EF. The derived EF in four different images over the study area showed, in general, good agreement with measured data.

Acknowledgements

The authors are grateful for the support provided by National Counsel for Scientific and Technological Development (CNPq) by providing scholarship to the first author.

References

Allen, R.G., Pereira, L.S., Raes, D., Smith, M. **Crop Evapotranspiration: Guidelines for Computing Crop Requirements**. Irrigation and Drainage Paper No. 56. FAO, Roma, Italy, 331p, 1998.

Bastiaanssen, W. G. M., Menenti, M., Feddes, R. A., Holtslag, A. A. A remote sensing surface energy balance algorithm for land (SEBAL): I. Formulation. **Journal of Hydrology**, v. 212–213, p. 198 – 212, 1998.

Bastiaanssen, W. G. M., Molden, D. J., Makin, I. W. Remote sensing for irrigated agriculture: examples from research and possible applications. **Agricultural Water Management**, v. 46, p. 137 – 155, 2000.

Chavez, J. L., Neale, C. M. U., Hipps, L. E., Prueger, J. H., Kustas, W. P. Comparing Aircraft-Based Remotely Sensed Energy Balance Fluxes Balance with Eddy Covariance Tower Data Using Heat Flux Source Area Functions. **Journal of Hydrometeorology**, v. 6, p. 923 – 940, 2005.

Colaizzi, P. D., Evett, S. R., Howell, T. A., Tolk, J. A. Comparison of Five Models to Scale Daily Evapotranspiration from One-Time-of-Day Measurements. **Transactions of the ASABE**, v. 49, p. 1409 – 1417, 2006.

Crago, R. Conservation and variability of the evaporative fraction during the daytime. **Journal of Hydrology**, v. 180, p. 173 – 194, 1996.

Crago, R., Brutsaert, W. Daytime evaporation and the self-preservation of the evaporative fraction and the Bowen ratio. **Journal of Hydrology**, v. 178, p. 241 – 255, 1996.

Farah, H. O., Bastiaanssen, W. G. M., Feddes, R. A. Evaluation of the temporal variability of the evaporative fraction in a tropical watershed. **International Journal of Applied Earth Observation and Geoinformation**, v. 5, p. 129 – 140, 2004.

Gentine, P., Entekhabi, D., Chehbouni, A., Boulet, G., Duchemin, B. Analysis of evaporative fraction diurnal behavior. **Agricultural and Forest Meteorology**, v. 143, p. 13 – 29, 2007.

Giolia, B., Migliettaa, F., Martinoa, B.D., Hutjesb, R.W.A., Dolmanc, H.A.J., Lindrothd, A., Schumachere, M., Sanzf, M.J., Mancag, G., Peressottih, A., Dumasi, E.J. Comparison between tower and aircraft-based eddy covariance fluxes in five European regions. **Agriculture and Forest Meteorology**, v. 127, p. 1 – 16, 2004.

Hoedjes, J. C. B., Chehbouni, A., Jacob, F., Ezzahar, J., Boulet, G. Deriving daily evapotranspiration from remotely sensed instantaneous evaporative fraction over olive orchard in semi-arid Morocco. **Journal of Hydrology**, v. 354, p. 53 – 64, 2008.

Kalthoff, N., Fiebig-Wittmaack, M., Meiβner, C., Kohler, M., Uriarte, M., Bischoff-Gauβ, I., Gonzales, E. The energy balance evapo-transpiration and nocturnal dew deposition of an arid valley in the Andes. **Journal of Arid Environments**, v. 65, p. 420 – 443, 2006.

Melesse, A. M., Frank, A., Nangia, V., Hanson, J. Analysis of energy fluxes and land surface parameters in a grassland ecosystem: a remote sensing perspective. **International Journal of Remote Sensing**, v. 29, p. 3325 – 3321, 2008.

Roerink, G. J.; Su, Z.; Menenti, M. S-SEBI: A Simple Remote Sensing Algorithm to Estimate the Surface Energy Balance. **Physical and Chemistry of Earth (B),** v.25, n.2, p.147-157, 2000.